CHARACTERIZATIONS OF BIOCOMPATIBLE AND BIOACTIVE HYDROXYAPATITE PARTICLES

M. N. Salimi[1], A. Anuar[2]

[1,2]School of Bioprocess Engineering,
Universiti Malaysia Perlis (UniMAP), Jejawi, Perlis

ABSTRACT

Mathematics is a beautiful subject with logic applications. However, the most common gene vectors used are virus based (viral gene vectors). These possess high immunological risk, so a non-viral gene vector maybe preferable. Nanocrystalline hydroxyapatite, HAp [$Ca_{10}(PO_4)_6(OH)_2$] is an example of a possible non-viral gene vector. This is due to its good biocompatibility, bioactivity and proven results as a non-viral gene vector. The HAp particles produced in this study was by the sol-gel method and the processing conditions were varied in terms of the processing temperatures (20°C, 30°C or 40°C) and the stirring rates (200 rpm, 400 rpm or 600 rpm). The particles formed from all of the processing conditions were systematically characterized and compared to each other. The characterizations performed were FTIR, for identifying functional groups, XRD for phase composition, crystallinity and particle size estimation (by applying Scherrer's formula) and SEM for surface morphology.The characterizations data obtained showed that the functional groups, phase composition, crystallinity and surface morphology were similar for all of the samples, the only difference being on the calculated particle size. It also showed that, at a lower processing temperature and higher stirring rate, smaller particle sizes were formed.

KEYWORDS*: Particle characterizations, Hydroxyapatite, XRD*

1.0 INTRODUCTION

Calcium phosphates are of interest for many biomedical applications due to their good biocompability and bioactivity (Figure 1). Hydroxyapatite (HAp) has been used as implant coating (Sun et al., 2001) and substitutes (Ramay & Zhang, 2004). Also, calcium phosphate nanoparticles have a range of applications in a number of fields, such as drug delivery, gene therapy (Figure 2), bone cements, dental applications, chromatography and waste water remediation. Each application has a need for the nanoparticles to be of a particular size

Corresponding author email: nabil@unimap.edu.my

range. There are various techniques reported in the literature for the production of nanosized calcium phosphate particles. These include wet chemical precipitation (Degirmenbasi et al., 2006), sol-gel synthesis (Kalita & Bhatt, 2007), hydrothermal synthesis (Pushpakanth et al., 2008), mechano-chemical synthesis (Wang et al., 2002) and several other methods by which nanoparticle of various shapes and sizes can be obtained.

Amorphous calcium phosphate (ACP) are used as remineralisation agents both in-situ (Tung et al., 1997) and in tooth restorative materials (Skrtic et al., 2004). Dicalcium phosphate anhydrous (DCPA) and dicalcium phosphate dehydrate (DCPD) (Brown & Chow, 1986), octacalcium phosphate (OCP) (Bermudez et al., 1994) and other calcium phosphate compounds (Mejdoubi et al., 1994; Ginebra et al., 1997; Lee et al., 1999) are used either as components or form as products of calcium phosphate bone cements.

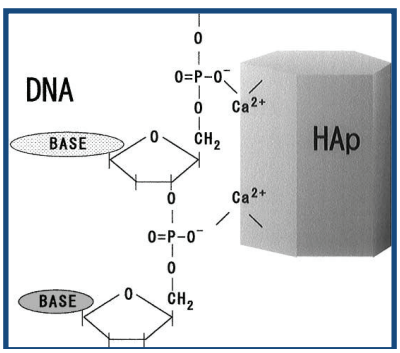

Figure 1. Schematic model of an affinity binding between a nHAp crystal and DNA (L. Sun et al., 2001)

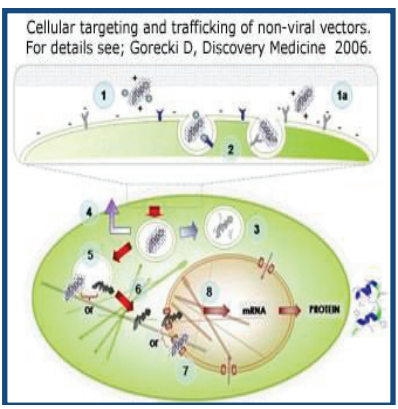

Figure 2. Mechanism of cellular uptake of non-viral gene vectors (via endocytosis)

Previous studies on nano-calcium phosphates have focused almost exclusively on nano-HAp, primarily because it is considered as a prototype of bioapatites, which are in nano-crystalline forms (LeGeros, 1991). Most of these preparations were done in a solution environment, such as chemical precipitation (Tas, 2000), sol-gel (Chai et al., 1999; Layrolle et al., 1998), microemulsion (Bose et al., 2003; Lim, 1999), electro-deposition (Shirkhanzadeh, 1998), and mechanochemical preparation followed by hydrothermal treatment (Suchanek et al., 2004). These methods generally can be used for preparing nano-HAp only because HAp is the least soluble calcium phosphate under most solution conditions; hence it is the phase that would form exclusively (Dorozhkin, 2007). Nanoparticles of the more soluble calcium phosphate phases, such as monocalcium phosphate monohydrate (MCPM), dicalcium phosphate monohydrate (DCPA), dicalcium phosphate dehydrate (DCPD), octacalcium phosphate (OCP), and amorphous calcium phosphate (ACP) have not been prepared by these methods.

The technique of calcium phosphate co-precipitation with plasmid DNA (pDNA) for in vitro transfection is used as a routine laboratory procedure (James & Grosveld, 1987). This method relies heavily on the fact that divalent metal cations, such as Ca^{2+}, Mg^{2+}, Mn^{2+}, and Ba^{2+} can form ionic complexes with the helical phosphates of DNA (Bloomfield, 1997; Truong-Le, 1999). Calcium phosphate can therefore form complexes with the nucleic acid backbone and thus may impart a stabilising function to certain DNA structures. DNA is reported to bind with HAp particles by the strong affinity between the phosphate groups of the DNA, which are negatively charged and the calcium ions of HAp (Okazaki et al., 2001). Calcium has a small hydrodynamic radius and therefore a high charge-to-surface area (Kulkarni et al., 2006). The complexes can then be carried across cell membrane via ion channel mediated endocytosis (Truong-Le et al., 1999). The specificity of calcium over other divalent metals is because it not only effectively condenses DNA, but does it in such a way that it is still functional following successful delivery to the cell nucleus, which is a result of Coulombic interactions (Walters & Welsh, 1999). Calcium phosphate has been used to effectively transfect bone tissue in vivo recently (Kuroda et al., 2005 & Endo et al., 2006).

Specific characteristics of particles (size, shape, surface, crystal structure and morphology) are among the important factors needed to control technological and biopharmaceutical properties of drug products. In general, morphology (crystal habit) can influence the physical and chemistry stability of solid dosage forms, a narrow size distribution is important to obtain content uniformity, while spherical particles

allow good flowability and tablettability. Furthermore, micronisation increases the surface area with a consequent increase of dissolution rate and bioavailability of the drug, thus promoting the formulation of active principle ingredients which may be insoluble or slightly soluble in aqueous media.

2.0 EXPERIMENTAL METHOD

A stoichiometric amount of aqueous solution of calcium nitrate tetrahydrate [$Ca(NO_3)_2.4H_2O$] was used and mixed with aqueous solution of ammonium phosphate [$(NH_4)_3PO_4$] with the molar ratio of 10:6 by using a peristaltic pump into a stirred beaker. This Ca/P molar ratio is the desired Ca/P ratio as observed in HAp. In mixing step, the processing conditions were varied in terms of the processing temperatures (20^oC, 30^oC or 40^oC) and the stirring rates (200 rpm, 400 rpm or 600 rpm). The concentrations of both precursors, which were the calcium nitrate tetrahydrate and ammonium phosphate and also stirring duration were constant. Then, in filtration step, HAp particles were filtered using a 0.22 μm filters. The filtered samples were then dried at a temperature of 100^oC and the drying step was carried out for 24 hour. Lastly, the dried samples were crushed using a pastle and mortar apparatus for 5 minutes. The procedure for the production of nanoparticles is outlined in Figure 3.

The particles formed from all of the processing conditions were systematically characterized and compared to each other. The characterizations performed were FTIR, for identifying functional groups, XRD for phase composition, crystallinity and particle size estimation (by applying Scherrer's formula) and SEM for surface morphology.

In the post co-precipitation of HAp particles from the sol-gel technique, the concentration of pDNA used was 50 mg/L. 10 μg (2μl) of pDNA from a stock solution of 5 g/L was dissolved in 198 μl of TE-$CaCl_2$ buffer (Tris-EDTA), giving a final volume of 200 μl. This solution was then mixed with 150 μg of HAp samples for each, which was vortexed for 15 seconds. The HAp-pDNA complex was incubated for 10 minutes at room temperature. Each post co-precipitation attachment of pDNA was repeated for 6 times.

In the gel electrophoresis procedure, Tris/Borate/EDTA (TBE), the running buffer for separating the pDNA was used. This buffer contained a mixture of 90 mM Tris, 90 mM boric acid and 2 mM EDTA at pH 8,

which was made up a 5x concentration stock. The running buffer of 0.5x was prepared by diluting 100 ml of the 5x concentration stock into a 1 L volumetric flask with distilled water (dH2O). 1% agarose matrix was prepared by dissolving 1 gram of agarose Type II powder in 100 ml of 1x TBE buffer and the agarose solution was poured into the gel rack container. The wells/slots were prepared by inserting a comb at one side of the agarose matrix, located about 5 - 10 mm from the end of the gel rack container. The agarose matrix was let to set for 30 minutes. Once it became solid, it was put into the electrophoresis tank, and 0.5x TBE running buffer (500 ml) was poured until the agarose matrix was completely submerged under the running buffer solution.

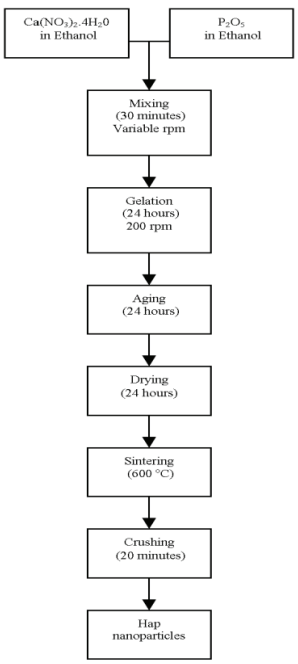

Figure 3. Flow chart of the sol-gel synthesis of hydroxyapatite powder

The wells were then filled with pDNA loaded HAp samples and pDNA marker was filled at the first well as reference of the pDNA molecular weight size. The electrophoresis measurements were undertaken at 75 volt (V) for 1 hour. When the electrophoresis measurement has stopped, the gel matrix was transferred into a container and ethidium bromide was poured to stain the pDNA for 45 minutes. The gel was washed several times with distilled water. Lastly, the gel was placed in an Ultraviolet Transilluminator device and images were taken using the Kodak UV Imagersoftware.

In-vitro transfection studies of hydroxyapatite – plasmid DNA (HAp-pDNA) post co-precipitation on two cell cultures, the NIH/3T3 fibroblasts and MC3T3 osteoblasts are also carried out. This transfection investigation was carried out as to evaluate the effectiveness of the HAp-pDNA complexes as pDNA carrier into the cells.

3.0 RESULTS & DISCUSSION

Phosphate and hydroxide absorption peaks for HAp were seen in the FTIR spectra (Figure 4). The formation of hydroxyapatite was denoted by the broad phosphate band centered from about 1000 to 1100 cm^{-1} (Varma & Babu, 2005) with bands at 960 to 965 cm^{-1} and 565 to 601 cm^{-1}, which corresponded to the $PO4^{3-}$ ion (Kawata et al., 2004; Miyaji et al., 2005). Major peaks for the phosphate group were between 1100 cm^{-1} to 960 cm^{-1} and 601 cm^{-1} to 567 cm^{-1}.

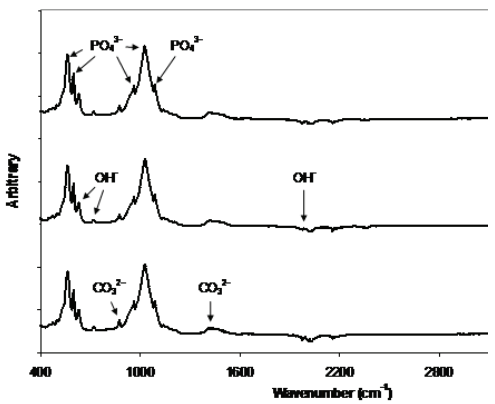

Figure 4. The FTIR spectra for hydroxyapatite samples prepared at 200, 400, 600 rpm and 30°C

The bands assigned to the stretching modes of hydroxyl groups in hydroxyapatite were seen at 1800 cm^{-1}, 632 cm^{-1} and 474 cm^{-1} (Varma et al., 2005; Kawata et al., 2004). The stretching modes of the carbonyl from the carbonate groups have been reported to be at 1550 cm^{-1}, 1457 cm^{-1} and 880 cm^{-1} for type A substitution, and 1462 cm^{-1}, 1418 cm^{-1} and 876 cm^{-1} for type B substitution (Krajewski et al., 2005). The hydroxyapatite formed in this study was type B substitution, where by carbonate ions substituted some of the phosphate ions in the apatitic structure. The source of carbonate would have originated from CO_2 in the atmosphere. The presence of type B carbonate in the apatite lattice has been shown to cause an increase in solubility both in vitro and in vivo tests (Krajewski et al., 2005). The FTIR spectra obtained for

all of the HAp samples showed that they are all the same, whereby processing conditions does not effect on particle composition.

The formation of hydroxyapatite was indicated by the characteristic peak occurring at $2\theta = 31.8^{o}$ which appeared on all of the HAp samples (Shimbayashi et al., 1995) and was verified by the pattern for HAp from the JCPDS catalogue. The narrow peaks in the XRD spectra indicate a high degree of crystallinity in the hydroxyapatite particles. After sintering at 600°C, no other phase besides hydroxyapatite was identified. The XRD patterns obtained for all of the HAp samples showed that they are all the same, whereby processing conditions does not effect on the resultant phase (Figure 5).

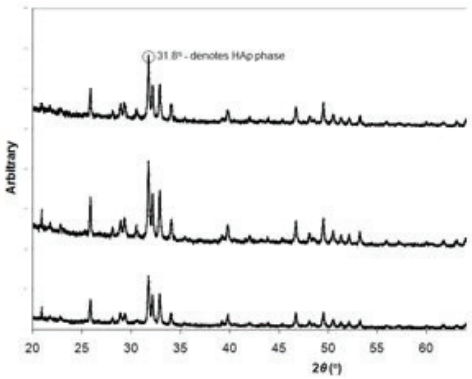

Figure 5. The XRD patterns for hydroxyapatite samples prepared at 200, 400, 600 rpm and 30°C

Particle size estimations by applying Scherrer's formula were shown to be in the nanosized range. SEM images of HAp nanoparticles showed that the particles formed agglomerates of approximately < 1 to 5 μm (Figure 6).

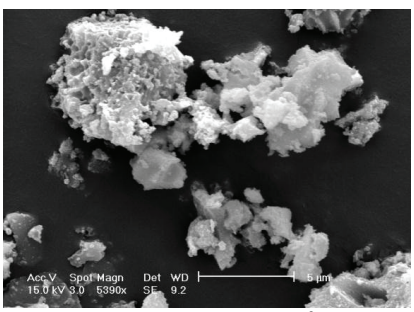

(a) 200 rpm & 20°C

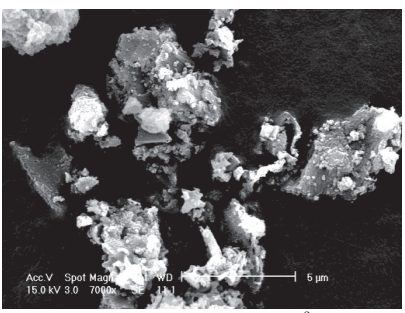

(b) 600 rpm & 30°C

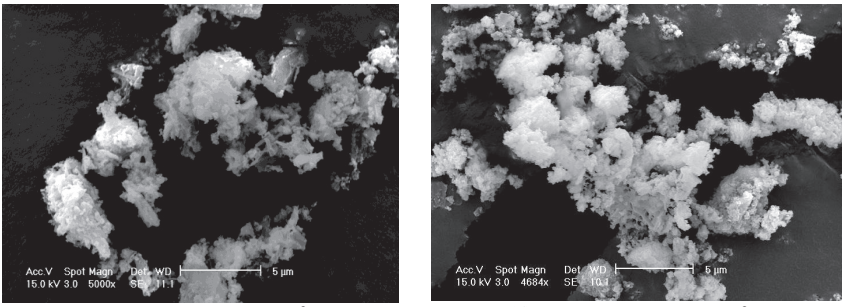

(c) 200 rpm & 20°C (d) 600 rpm & 30 °C

Figure 6. The SEM images for hydroxyapatite samples prepared at 200 & 600 rpm and 20 & 30°C

The gel for the HAp-pDNA attachment showed the presence of pDNA on/within the particles by the bands on the gel. These are clearly shown in Figure 7. The pDNA molecular weight used in these studies can be determined from the pDNA standard molecular weight ladder (shown on Lane 1). The molecular weight of the pDNA used is 5757 base pair (5.7 kb) shown by the position of the last strip of the band (representing the open circular pDNA), which is located between the 5 kb and 6 kb of the standard pDNA ladder. Many previous studies by other groups have showed the efficiency of post co-precipitation, for example James et al. (1987), Truong-Le (1999) and Elliott (1994) and Jordan et al. (1996) reported that HAp-pDNA co-precipitates can arise spontaneously in supersaturated solutions, but only in a narrow range of physico-chemical conditions, with principally the calcium and phosphate concentrations being the most significant.

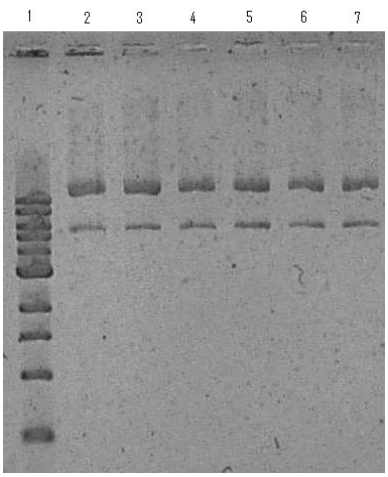

Figure 7. Gel electrophoresis of HAp post co-precipitation with pDNA for HAp particles produced by sol-gel method

Transfection was detected by fluorescence microscopy after the incubation of the NIH/3T3 fibroblast and MC3T3 osteoblast cell lines with the HAp-pDNA complexes. From the GFP expression observed by the fluoresence microscopy, it was noted that all of the HAp-pDNA complexes were taken up by both cell lines and the gWiz-GFP pDNA mammalian expression vector encoding green fluorescent protein fluoresced under the fluorescence microscope. The fluorescence light micrographs of some of the transfected CaP-pDNA complexes in the NIH/3T3 fibroblast and MC3T3 osteoblast cell lines are shown in Figure 8. The green fluorescence indicates the pDNA uptake by the cells and subsequently the GFP expression.

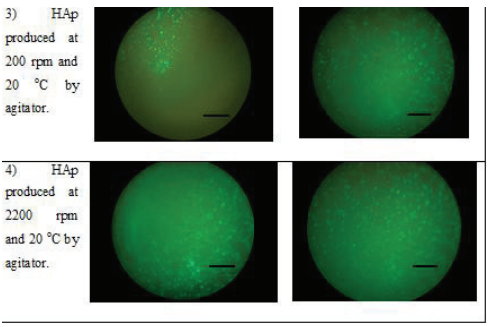

Figure 8. Fluoresence light micrographs of the NIH/3T3 fibroblast and MC3T3 osteoblast cell lines transfected with some of the HAp-pDNA complexes (scale bar unit is 250 μm). The green fluorescence indicates the pDNA uptake by the cells and subsequently the GFP expression

4.0 CONCLUSION

The characterizations data obtained showed that the functional groups, phase composition, crystallinity and surface morphology were similar for all of the samples, the only difference being on the calculated particle size. It also showed that, at a lower processing temperature and higher stirring rate, smaller particle sizes were formed.

The HAp-pDNA complexes were shown to be a reliable transfection vector in both the NIH/3T3 fibroblast and MC3T3 osteoblast cell lines. The HAp-pDNA complexes were readily taken up by the cells as shown by the fluorescence light micrographs.

5.0 REFERENCES

Bermudez, O., Boltong, G. M., Driessens, F. C. M., Planell, J. A. (1994). Development of an octacalcium phosphate cement. *J. Mater. Sci. Mater. Med., 5*, 144 – 146.

Bloomfield, V. A. (1997). DNA condensation by multivalent cations. *Biopolymers 44*(3), 269 – 282.

Bose, J., Saha, S. K. (2003). Synthesis and characterization of hydroxyapatite: nanopowders by emulsion technique. *Chem. Mater., 15*, 4464 – 4469.

Brown, W. E., & Chow, L. C. (1986). Cements research progress. *American Ceramic Society*, 352 – 379.

Chai, C. S., Ben-Nissan, B. (1999). Bioactive nanocrystalline sol-gel hydroxyapatite coatings. *J. Mater. Sci. Mater. Med., 10*, 465 – 469.

Degirmenbasi, N., Kaylon, D. M., & Birinci, E. (2006). Biocomposites of nanohydroxyapatite with collagen and poly(vinyl alcohol). *Colloids. Surf B.*, 48, 42 – 49.

Dorozhkin, S. V. (2007). Calcium orthophosphates. *J. Mater. Sc., 42* ,1061-1095.

Elliot, J. C. (1994). *Structure and Chemistry of the Apatites and Other Calcium Orthophosphates.* Amsterdam: Elsevier.

Endo, M., Kuroda, S., Kondo, H., Maruoka, Y., Ohya, K., & Kasugai, S. (2006). Bone regeneration by modified gene-activated matrix: Effectiveness in segmental tibial defects in rats. *Tissue Engineering, 12*(3), 489 – 497.

Ginebra, M. P., De Fernandez, E., Maeyer, E. A. P., Veerbeck, R. M. H., Boltong, M. G., Ginebra, F., Driessens, F. C. M., & Planell, J. A. (1997). Setting reaction and hardening of an apatitic calcium phosphate cement. *J. Dent. Res., 76*, 905 – 912.

James, R. F. L., Grosveld, F. G. (1987). Techniques in molecular biology. Walker, *J. M., Gaastra, W. (*Eds.), (pp. 187 – 202).

Jordan, M., Schallhorn, A., & Wurm, F. M. (1996). Transfecting mammalian cells: optimization of critical parameters affecting calcium-phosphate precipitate formation. *Nucleic Acids Res., 24*, 596 – 601.

Kalita, S. J., & Bhatt, H. A. (2007). Nanocrystalline hydroxyapatite doped with magnesium and zinc: synthesis and characterization. *Mater. Sci. Eng., 27*, 837 – 848.

Kawata, M., Uchida, H., Itatani, K., Koda, I., Okada, S., & Aizawa, M. (2004). Development of porous ceramics with well-controlled porosites and pore sizes from apatite fibers and their evaluations. *J. Mater. Sci. Mater. Med.*, 817 – 823.

Krajewski, A., Mazzocchi, M., Ravaglioli, P. L., Buldini, A., Tinti, A., Taddei, P., & Fagnano, C. (2005). Synthesis of carbonated hydroxyapatites:

efficiency of the substitution and critical evaluation of analytical methods. *Journal of Molecular Structure,* 221 – 228.

Kulkarni, V. I., Shenoy, V. S., Dodiya, S. S., Rajyaguru, T. H., & Murthy, R. R. (2006). Role of calcium in gene therapy. *Expert opinion on Drug Delivery., 3*(2), 235 – 245.

Kuroda, S., Kondo, H., Ohya, K., & Kasugi, S. (2005). A new technique with calcium phosphate precipitate enhances efficiency of in vivo plasmid DNA gene transfer. *Journal of Pharmacological Sciences, 97*(2), 227 – 233.

Layrolle, P., Ito, A., & Tateishi, T. (1998). Sol-gel synthesis of amorphous calcium phosphate and sintering into microporous hydroxyapatite bioceramics. *J. Amer. Ceram. Soc., 8*,1421 – 1428.

Lee, D. D., Tofighi, A., Aiolova, M., Chakravarthy, P., Catalano, A., Majahad, A., & Knaack, D. (1999). A biomimetic bone substitute and drug delivery vehicle. *Clin. Orthop. Suppl.*,367.

LeGeros, R. Z. (1991). Calcium Phosphates in Oral Biology and Medicine. Karger, Basel, Myers, H. M. (Eds.), (pp. 110 – 118).

Lim, G. K., Wang, J., Ng, S. C., Gan, L. M. (1999). Nanosized hydroxyapatite powders from microemulsions and emulsions stabilised by a biodegradable surfactant. *J. Mater. Chem.*, 9, 1635.

Mejdoubi, E., Lacout, J.L., Heughebaert, J. C., Michaud, P. (1994). Optimization of a hydraulic calcium phosphate cement. *Adv. Mater. Res*. ,163 – 171.

Miyaji, F., Kono, Y., Suyama, Y. (2005). Formation and structure of zinc-substituted calcium hydroxyapatite. *Mater. Res. Bull., 4*0, 209 – 213.

Okazaki, M., Yoshida, Y., Yamaguchi, S., Kaneno, M., & Elliot, J. C. (2001). Affinity binding phenomena of DNA onto apatite crystals. *Biomaterials, 22,* 2459 – 2464.

Pushpakanth, S., Srinivasan, B., Sreedhar, B., & Sastry, T. P. (2008). An in-situ approach to prepare nanorods of titania-hydroxyapatite (TiO2-HAp) nanocomposite by microwave hydrothermal technique. *Mater. Chem. Phys*., 107, 492 – 498.

Ramay, H. R. R., & Zhang, M. (2004). Biphasic calcium phosphate nanocomposite porous scaffolds for load-bearing bone tissue engineering. *Biomaterials., 25*, 5171 – 5180.

Shimbayashi, S., Hashimoto, N., Kawamura, H., & Uno, T. (1995). Mineral Scale Formation and Inhibition. In Amjad, Z. (Ed.), (pp. 14 – 15). New York: Plenum Press.

Shirkhanzadeh, M. (1998). Direct formation of nanophase hydroxyapatite on cathodically polarized electrode. *J. Mater. Sci. Mater. Med.*, 9 , 67 – 72.

Skrtic, D., Antonucci, J. M., Eanes, E. D., & Eidelman, N. (2004). Dental composites based on hybrid and surface-modified amorphous calcium phosphates. *Biomaterials, 25*, 1141 – 1150.

Suchanek, W. L., Byrappa, K., Shuk, P., Riman, R. E., Janas, V. F., Ten Huisen, K. S. (2004). Mechanochemical-hydrothermal synthesis of calcium phosphate powders with coupled magnesium and carbonate substitution. *J. Solid State Chem.*, 177, 793 – 799.

Sun, L., Berndt C. C., Kucuk, A., & Gross, K. A. (2001). Material fundamentals and clinical performance of plasma sprayed hydroxyapatite coatings. Review, *Appl. Biomat., 58* (5), 570 – 592.

Tas, A. C. (2000). Combustion synthesis of calcium phosphate bioceramic powders. *J.Eur. Ceram. Soc*., 20, 2389.

Truong-Le, V. L., Walsh, S.M., Mao, E., Schwabert, H. Q, Guggino, W. B., August, J. T., Leong, K. W. (1999). Gene transfer by DNA-Gelstin nanospheres. *Arch. Biochem. Biophys*., 47 - 56.

Tung, M., Eichmiller, F., Gibson, H., Ly, A., Skrtic, D., & Schumacher, G. (1997). Dentin Desensitization by in situ Formulation of Calcium Phosphate. *J. Dent. Res*., 76 , 2985.

Varma, H., Babu, S. S. (2005). Synthesis of calcium phosphate bioceramics by citrate gel pyrolysis method. *Ceram. Int.,* 31, 109 – 114.

Walters, R. W., Welsh, M. J. (1999). Mechanism by which calcium phosphate coprecipitation enhances adenovirus-mediated gene transfer. *Gene Therapy.,* 6(11), 1845 – 1850.

Wang, L., Nemoto, R., & Senna, M. (2002). Microstructure and chemical states of hydroxyapatite/silk fibroin nanocomposites synthesized via a wet mechanochemical route. *J. Nanopart. Res.*, 4, 535 – 540.